High-Resolution Magnetometry with a Spinor Bose-Einstein Condensate

M. Vengalattore,[1] J. M. Higbie,[1] S. R. Leslie,[1] J. Guzman,[1] L. E. Sadler,[1] and D. M. Stamper-Kurn[1,2]

[1]*Department of Physics, University of California, Berkeley California 94720, USA*

[2]*Materials Sciences Division, Lawrence Berkeley National Laboratory, Berkeley, California 94720, USA*

(Received 15 December 2006; published 17 May 2007)

We demonstrate a precise magnetic microscope based on direct imaging of the Larmor precession of a ^{87}Rb spinor Bose-Einstein condensate. This magnetometer attains a field sensitivity of 8.3 pT/Hz$^{1/2}$ over a measurement area of 120 μm^2, an improvement over the low-frequency field sensitivity of modern SQUID magnetometers. The achieved phase sensitivity is close to the atom shot-noise limit, estimated as 0.15 pT/Hz$^{1/2}$ for a unity duty cycle measurement, suggesting the possibilities of spatially resolved spin-squeezed magnetometry. This magnetometer marks a significant application of degenerate atomic gases to metrology.

DOI: 10.1103/PhysRevLett.98.200801 PACS numbers: 07.55.Ge, 03.75.Mn

Precision magnetometers that map magnetic fields with high spatial resolution have been applied to studies of condensed matter systems [1], biomagnetic imaging [2], and tests of fundamental symmetries [3]. Many of these applications require the measurement of magnetic fields at low ($<$10 Hz) frequencies. Current technologies capable of micron-scale magnetic microscopy include superconducting quantum interference devices (SQUIDs), scanning Hall probe microscopes, magnetic force microscopes, and magneto-optical imaging techniques [4]. Of these, SQUIDs offer the highest sensitivity, demonstrated at 30 pT/Hz$^{1/2}$ over a measurement area of around 100 μm^2 [5]. The low-frequency sensitivity of these devices is limited by $(1/f)$ flicker noise of unknown origins [6].

Magnetic fields may also be sensed by detecting the Larmor precession of spin-polarized atomic gases. To date, atomic magnetometers have achieved field sensitivities of 0.5 fT/Hz$^{1/2}$ over measurement volumes of 0.3 cm^3 [7]. However, attaining high spatial resolution with a hot-vapor medium is precluded by rapid thermal diffusion of the atoms, restricting the minimum resolved length scale of these magnetometers to around 1 mm.

Trapped ultracold gases present an attractive medium for a variety of precision measurements due to their negligible Doppler broadening and long coherence times [8–10]. Spinor Bose gases, composed of atoms with a spin degree of freedom, are particularly well suited to magnetic microscopy. Unlike in hot-vapor atomic magnetometers, the suppression of thermal diffusion in a gas through Bose condensation enables precise measurements at high spatial resolution. Also, density-dependent collision shifts, which deleteriously affect other types of precision measurements using dense ultracold gases, do not affect Larmor precession due to the rotational invariance of interparticle interactions in a spinor gas [9,11].

Here, we perform precise magnetic microscopy with high two-dimensional spatial resolution using a ^{87}Rb $F = 1$ spinor Bose-Einstein condensate (BEC). In our magnetometer, longitudinally spin-polarized spinor condensates are prepared in an optical trap. Larmor precession is induced using a rf pulse to tip the magnetization perpendicular to a bias field imposed along the axis of the condensate. The spins in each region of the condensate then precess at a rate that is proportional to the *local* magnetic field. After a variable integration time, the condensate is probed using magnetization-sensitive imaging to extract the local Larmor phase. The *difference* in this phase between various regions of the condensate reveals the spatial variation of the magnetic field.

The determination of the accrued Larmor phase of a coherent spin state, such as the transversely magnetized condensate, is subject to an uncertainty in the initial phase of $\delta\phi_a = 1/\sqrt{N}$ due to projection noise of measuring N atoms. This noise limits the field sensitivity over a measurement area A to $\delta B = (\hbar/g\mu_B)(1/\sqrt{\tau DT})(1/\sqrt{\tilde{n}A})$, where τ is the Zeeman coherence time and $\tilde{n}$ the local column density of the gas. We assume the measurement is repeated over a total time T at a duty cycle D. The $A^{-1/2}$ scaling of field sensitivity with the measurement area for the atomic magnetometer may be compared with the area scaling for SQUID magnetometers. This scaling ranges between $A^{-3/4}$, for a fixed SQUID sensor coupled optimally to a variable pickup loop, and $A^{-5/8}$, for direct sensing with a SQUID optimized to operate at the quantum limit for the noise energy [12]. In either case, the atomic magnetometer outperforms SQUID magnetometers at small measurement areas (Fig. 1).

Optical detection of Larmor precession is limited also by photon shot noise. In this work, the Larmor precession phase is measured by repeated phase-contrast imaging of the condensate using circular polarized light [9]. For our probe detuning of $\Delta = 2\pi \times 500$ MHz below the $F = 1 \rightarrow F' = 2$ (D1) transition of ^{87}Rb, the phase-contrast signal can be written as $s \simeq 1 + 2\tilde{n}\sigma_0(\gamma/2\Delta) \times [c_0 + c_1\langle F_y\rangle]$, where $\sigma_0 = 3\lambda^2/2\pi$ is the resonant cross section, γ is the natural linewidth, and F_y is the projection of the local atomic spin on the imaging axis $\hat{y}$, which is perpendicular to the field axis. The detuning-dependent

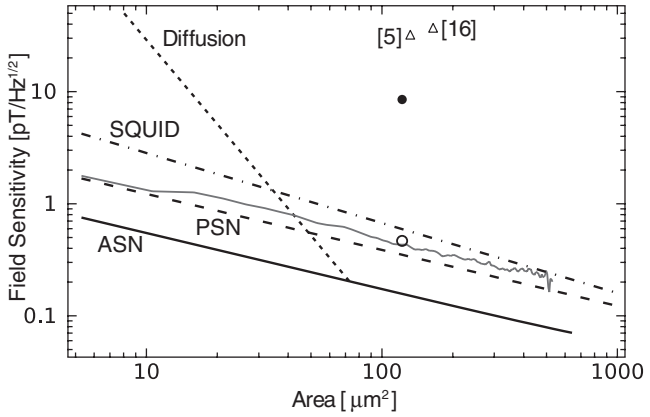

FIG. 1. Field sensitivity for repeated measurements using the spinor BEC magnetometer. Curves marked ASN (PSN) represent atom (photon) shot-noise limited sensitivities, assuming $\tau = 250$ ms, $D = 1$, and the atomic column density and probe light levels for our experiment. Diffusion of magnetization limits the sensitivity for a given length scale by imposing a limit on τ (short dashed line, assuming $D = 1$). The gray line indicates the measured spatial root Allan variance; the sensitivity demonstrated in measurements of an optically induced magnetic field (see text), assuming duty cycles of $D = 0.003$ (●) or $D = 1$ (○), is also shown. Results are compared both to the ideal sensitivity of a quantum-limited SQUID magnetometer (dot-dashed line) and to demonstrated low-frequency sensitivities [5,16] (△).

constants $c_0 = 0.118$ and $c_1 = 0.274$ describe the isotropic polarizability and optical activity, respectively. We neglect the effects of linear birefringence ($\propto \langle F_y^2 \rangle$). The Larmor precession phase is estimated by tracking the sinusoidal oscillation of the phase-contrast signal across the sequence of phase-contrast images. The photon shot-noise limited sensitivity of this estimate is then $\delta\phi_\gamma \approx \sqrt{(2/\eta N_p)}[\sqrt{1 + \tilde{n}\sigma_0(\gamma/2\Delta)c_0}/\tilde{n}\sigma_0(\gamma/2\Delta)c_1]$, limiting the field sensitivity to $\delta B = (\hbar/g\mu_B)(\delta\phi_\gamma/\sqrt{\tau DT})$. Here, η is the detection quantum efficiency and N_p is the total photon fluence, integrated across the multipulse imaging sequence, within the region of interest.

For our demonstration, spin-polarized ^{87}Rb condensates of up to 1.4×10^6 atoms were confined in a single-beam optical dipole trap characterized by trap frequencies $(\omega_x, \omega_y, \omega_z) = 2\pi(165, 440, 4.4)$ s^{-1} [9]. The tight confinement along the imaging axis (condensate radius $r_y = 2.0$ μm) ensured that the condensate is effectively two dimensional with respect to spin dynamics. Next, we applied a $\sim$100 μs resonant rf pulse at 115 kHz to rotate the magnetization perpendicular to the $\hat{z}$ axis. The sample was then allowed to Larmor precess in the presence of a 165(7) mG bias field aligned along its long axis ($\hat{z}$). A measurement integration time of 250 ms was chosen; at longer times, measurements were hampered by uncontrolled motion of the condensate along the weakly confining dimension (see below).

We operated our ultracold-atom magnetometer under two testing conditions. In one, we assessed the measurement noise at short spatial length scales by measuring the long length-scale inhomogeneous background magnetic field in our apparatus. We applied a third-order polynomial fit to the measurements from each run of the magnetometer to account for this fluctuating background [13], and analyzed residuals from this fit to characterize experimentally the noise limits to our magnetometer.

In the second testing condition, we used the magnetometer to measure a deliberately applied, localized magnetic field. Such a field was simulated using a circularly polarized laser beam at a wavelength of 790 nm. The choice of wavelength and polarization ensured that this beam imposed a local optically induced Zeeman shift [14] on the trapped atoms [Fig. 2(a)]. The beam was aligned at an angle $\theta \sim 60°$ to the direction of the bias field, incident and focused in the plane perpendicular to the imaging axis. The magnetic background for each run of the magnetometer was again determined by third-order polynomial fits, but using measurements from regions far from the localized field. The magnitude of the localized field was extracted from the residuals of this fit.

Measurements of this simulated field were affected by small center-of-mass oscillations of the condensate along its long axis. An oscillation with amplitude δz blurs the magnetic landscape and washes out features smaller than δz. Unable to eliminate this motion, we monitored the condensate position for each run of the magnetometer by a sequence of 4 images spaced at a quarter period of the

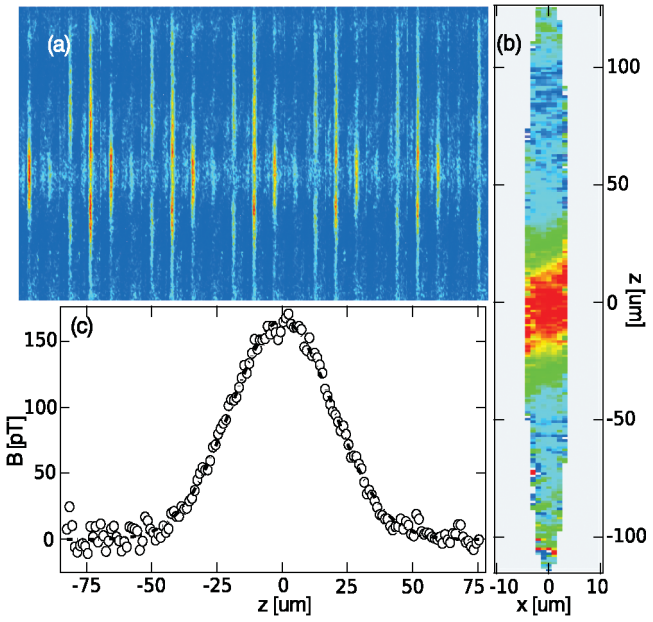

FIG. 2 (color). (a) A sequence of phase contrast images, taken at a strobe rate of 14 kHz, reveal Larmor precession as an aliased frame-to-frame oscillation of the signal. (b) The resulting 2D map of the magnetic field, obtained by a pixel-by-pixel estimation of the Larmor precession phase, reveals the optically induced local magnetic field near the condensate center. (c) The 1D phase profile precisely maps the applied field inhomogeneity with peak strength of 166.2 ± 1.2 pT.

axial trap frequency, taken prior to the Larmor imaging sequence. We discarded measurements in which the excursion was comparable to the extent of the localized field.

Two-dimensional maps of the magnetic field were obtained from a pixel-by-pixel analysis of the Larmor precession phase within the profile of the condensate [Fig. 2(b)]. The frame-to-frame variation of this signal showed the characteristic oscillations due to Larmor precession as well as an overall decay of the condensate number due to off-resonant scattering of probe light. This decay was taken into account in obtaining an unbiased estimate of the local Larmor phase. Our 2D approach was found to be susceptible to imaging aberrations, primarily in the narrow ($\hat{x}$) dimension of the gas.

More robust measurements were obtained by reducing measurements to a single resolved direction along the $\hat{z}$ axis. For this, the aberrated signal profile in the $\hat{x}$ direction was determined at each z coordinate in the images from averages over the multiple frames. The phase-contrast signal height in each image frame and at each z coordinate was then determined, effectively integrating the signal over $\hat{x}$. As before, the local Larmor phase was estimated by a least squares fit to the phase-contrast signal to obtain 1D phase profiles [Fig. 2(c)].

The demonstrated sensitivity of our magnetometer is shown in Fig. 1. The spatial root Allan variance [15] from the 1D data was determined for each of 15 runs of the magnetometer under the first testing conditions (background only) and then averaged. The measurement *area* is determined by accounting for the effective 5.3 μm length over which the aberrated signals are averaged in the $\hat{x}$ direction. The observed noise level agrees closely with photon shot noise estimates and is $\sim$3 times that due to atomic shot noise given the number of atoms in the corresponding areas. Excess noise for areas larger than about 20 μm^2 was found to correlate with the local intensity of the probe light, an effect we attribute to probe-light induced shifts of the Larmor frequency during imaging. This noise can be reduced further by using a linearly polarized probe with a more homogenous intensity profile and by carefully aligning the magnetic bias field to be normal to the imaging axis.

Results from measurements under the second testing condition (background plus localized field) are shown in Fig. 3. Here, the strength of the applied field (peak value of Gaussian fits) was measured repeatedly at several powers of the field-inducing laser beam. From these measurements, a calibration between the laser power and the localized field strength was obtained. From the residual scatter in measurements of field with strengths up to 60 pT, we determine the rms sensitivity of our Larmor precession phase measurements as 1.0×10^{-2} rad over the 120 μm^2 area under the Gaussian profile, corresponding to a single-shot field sensitivity of 0.9 pT. A marginally larger variance at higher fields points to the existence of small systematic effects, e.g., residual motion of the condensate or variations in the localized field strength.

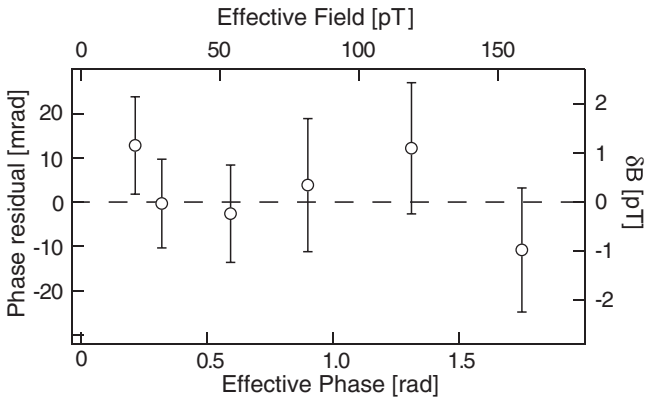

FIG. 3. Single-shot measurements of the localized magnetic field imposed by a laser beam focused to $\sigma = 24$ μm rms width. Residuals are shown from a linear calibration fit of the field magnitude versus laser power. Error bars indicate standard deviations for 10 measurements per setting.

Under repeated operation, our magnetometer, with a low duty cycle of just $D = 3 \times 10^{-3}$, attains a field sensitivity of 8.3 pT/Hz$^{1/2}$, an improvement over that demonstrated for low-frequency ($<$10 Hz) field measurements with modern SQUID magnetometers [5,16]. Plausible extensions of current cold-atom experimental methods should enable duty cycles of order unity. At full duty cycle, our single-shot sensitivity would yield a field sensitivity of 0.5 pT/Hz$^{1/2}$.

In the photon shot-noise limit, the sensitivity of an atomic magnetometer increases with increasing probe fluence. While calculations based on linear Raman scattering rates indicated that reliable phase estimates could be obtained even at a fluence of 3400 photons/μm^2, it was found that light-induced decay of our imaging signal far exceeded these predictions. The discrepancy was attributed to superradiant Raman scattering of atoms into the $F = 2$ hyperfine states, in which atoms are no longer observed by our probe. To counter this problem, we reduced the superradiant gain by lowering the probe intensity and divided the probe light shone on each frame of the imaging sequence into four pulses, each of duration 2.2 μs and spaced by the Larmor period of $\sim$10 μs. We also applied additional light during imaging that was resonant with the $F = 2 \rightarrow F' = 3$ (D2) transition so as to scatter light preferentially off the $F = 2$ atoms produced during superradiance and induce motional decoherence. Together, these strategies enabled a probe fluence of 750 photons/μm^2.

Our magnetometry medium, though Bose condensed, is still a gas in which atoms are free to move. Thus, in determining the phase shift accrued due to a local magnetic field, one must consider atomic motion due to both quantum-mechanical and classical effects. For instance, imposing a weak inhomogeneous field of characteristic length σ leads to quantum diffusive motion of the fluid. For times $\tau > \tau_Q = m\sigma^2/\hbar$, with m the atomic mass, the

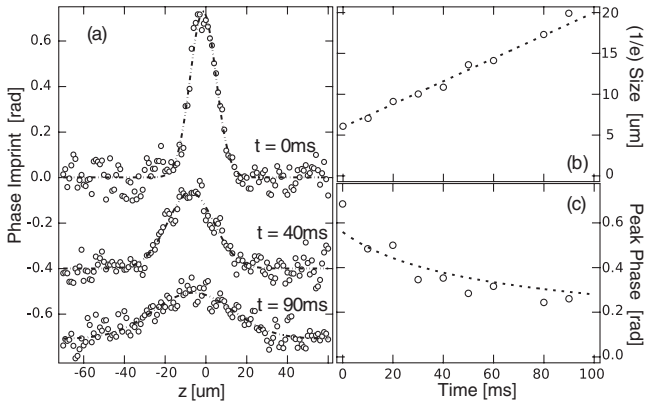

FIG. 4. Quantum evolution of an imprinted phase. (a) Cross sections of the phase imprint after free evolution times of $t = 0$, 40, and 90 ms. Traces are offset for clarity. (b) The $1/e$ width and (c) peak value of the imprinted phase are compared to (b) numerical simulations based on a noninteracting spinor gas and to (c) the expected scaling imposed by normalization of magnetization.

motion of the spinor gas will reduce the phase accrued due to Larmor precession. This evolution can be considered to be the quantum limit of thermal diffusion observed in NMR studies [17]. In our experiment, the condition $\tau = 250\ \mathrm{ms} > \tau_Q$ is reached at length scales below 10 μm (Fig. 1). For integration times $\tau \ll \tau_Q$, effects of quantum diffusion require that phase measurements ϕ be corrected by an amount $\delta\phi/\phi \sim (\tau/\tau_Q)^4$.

An inhomogeneous magnetic field also exerts forces on magnetic dipoles. In the extreme case of static inhomogeneous fields with a Zeeman energy comparable to the chemical potential ($\sim 10^5$ times larger than those studied in this work), these classical forces can visibly modify the density distribution of the condensate [18]. In our case, these forces result in small corrections and limits to the accrued Larmor phase. The field strength B and a characteristic length σ for its variation define a classical time scale $\tau_C = \sqrt{m\sigma^2/\mu_B B}$, the time taken by an atom to move σ when accelerated by this field. For an integration time τ, this classical motion imposes a limit on the maximum detectable phase shift (when $\tau = \tau_C$) of $\phi_m \simeq \tau_Q/\tau$. It should be noted that neither the diffusion of an imprinted phase nor the limitation on the dynamic range are fundamental; both can be eliminated by constraining atomic motion with suitable optical potentials.

To observe the dilution of magnetization due to atomic motion, we imposed a light-induced Zeeman shift localized to a $1/e$ width of 5.4 μm onto the transversely magnetized spinor condensate. Following a 5 ms exposure to the field-inducing laser beam, the condensate magnetization was allowed to evolve freely for variable time before being probed. During this evolution, the imprinted Larmor phase diminished in peak height and grew in extent, matching well with calculations based on a noninteracting spinor gas in a localized field (Fig. 4).

In conclusion, we have demonstrated a spinor-BEC magnetometer, a powerful application of ultracold atoms to precision measurement of scientific and technological significance. Inasmuch as the Larmor precession phase represents the phase relations among BECs in several Zeeman states, this magnetometer can be regarded as a condensate interferometer with high temporal and spatial resolution. The single-shot phase sensitivity and shot-to-shot variations of 10 mrad achieved here represent an order of magnitude improvement over the performance of previous BEC interferometers [19].

The demonstrated phase sensitivity is close to the atom shot-noise limit. This augurs spin-squeezed magnetometry via continuous quantum nondemolition measurements of the condensate [20] and novel spatially and temporally resolved studies of spin-squeezed ensembles.

We thank D. Budker and J. Clarke for helpful discussions. This work was supported by the NSF and the David and Lucile Packard Foundation. S. R. L. acknowledges support from the NSERC.

[1] C. C. Tsuei and J. R. Kirtley, Rev. Mod. Phys. **72**, 969 (2000).
[2] K. Kobayashi and Y. Uchikawa, IEEE Trans. Magn. **39**, 3378 (2003).
[3] L. R. Hunter, Science **252**, 73 (1991).
[4] S. J. Bending, Adv. Phys. **48**, 449 (1999).
[5] J. R. Kirtley *et al.*, Appl. Phys. Lett. **66**, 1138 (1995).
[6] R. H. Koch *et al.*, J. Low Temp. Phys. **51**, 207 (1983).
[7] I. K. Kominis *et al.*, Nature (London) **422**, 596 (2003).
[8] P. Treutlein *et al.*, Phys. Rev. Lett. **92**, 203005 (2004).
[9] J. M. Higbie *et al.*, Phys. Rev. Lett. **95**, 050401 (2005).
[10] N. Davidson *et al.*, Phys. Rev. Lett. **74**, 1311 (1995).
[11] T. L. Ho, Phys. Rev. Lett. **81**, 742 (1998); T. Ohmi and K. Machida, J. Phys. Soc. Jpn. **67**, 1822 (1998).
[12] R. H. Koch *et al.*, Appl. Phys. Lett. **38**, 380 (1981).
[13] Based on the geometry of the apparatus and the location of magnetic field sources, we estimate background field variations across the condensate due to fourth order and higher terms to be $\ll 1$ fT.
[14] J. Dalibard and C. Cohen-Tannoudji, J. Opt. Soc. Am. B **6**, 2023 (1989).
[15] The spatial Allan variance is similar to the commonly used temporal Allan variance [D. W. Allan, Proc. IEEE **54**, 221 (1966)], except that the data series (i.e., the magnetic field) is now a function of position rather than time.
[16] T. S. Lee *et al.*, Rev. Sci. Instrum. **67**, 4208 (1996).
[17] H. Carr and E. Purcell, Phys. Rev. **94**, 630 (1954).
[18] S. Wildermuth *et al.*, Nature (London) **435**, 440 (2005).
[19] S. Gupta *et al.*, Phys. Rev. Lett. **89**, 140401 (2002).
[20] A. Kuzmich *et al.*, Europhys. Lett. **42**, 481 (1998); J. M. Geremia *et al.*, Science **304**, 270 (2004).